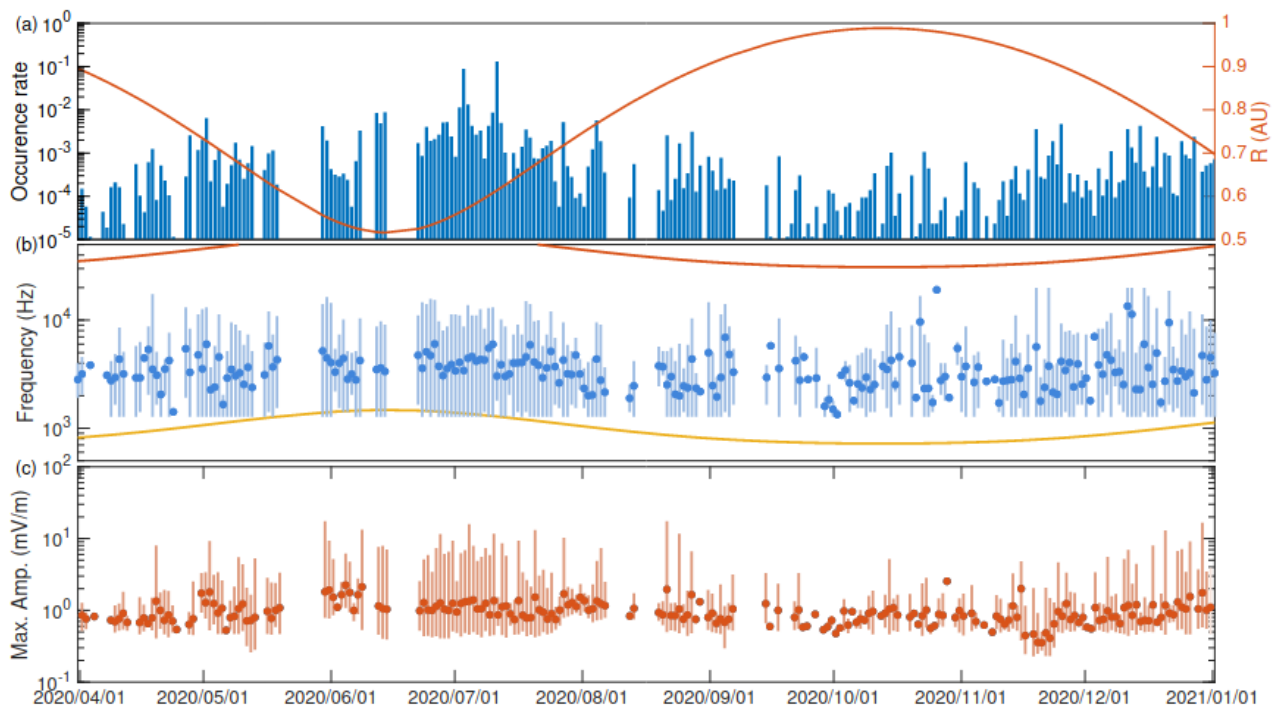


Results of the Department of Space Physics, Institute of Atmospheric Physics of the Czech Academy of Sciences, published in 2021

1. Plasma waves and interplanetary dust in the solar wind: new measurements of the Time Domain Sampler module within the Radio and Plasma Waves instrument onboard Solar Orbiter.

The Radio and Plasma Waves instrument, including the Time Domain Sampler, has been measuring electromagnetic phenomena in the solar wind nearly continuously since the start of Solar Orbiter in February 2020. Data from the Czech instrument, obtained at a range of heliocentric distances, resulted in several studies of high frequency waves in the solar wind plasma and a study of interplanetary dust, deriving for the first time the average radial velocity of dust grains.



Wave emission observed by the Time Domain Sampler of the Radio and Plasma Waves instrument onboard Solar Orbiter: (a) blue bars show the occurrence rate of intense waves below 20 kHz, overplotted orange line representing the distance from the Sun; (b) distribution of observed wave frequencies with their observed minimum-maximum range, orange and yellow lines respectively represent modelled electron and proton plasma frequencies; (c) averaged maxima of wave amplitudes with their range.

References:

J. Souček, D. Piša, I. Kolmašová, L. Uhlíř, R. Lán, O. Santolík, V. Krupař, O. Krupařová, J. Baše, M. Maksimovic, S. D. Bale, T. Chust, Yu. V. Khotyaintsev, V. Krasnoselskikh, M. Kretzschmar, E. Lorfèvre, D. Plettemeier, M. Steller, Š. Štverák, A. Vaivads, A. Vecchio, D. Bérard and X. Bonnin, Solar Orbiter Radio and Plasma Waves – Time Domain Sampler: In-flight performance and first results, A&A, 656 (2021) A26, <https://doi.org/10.1051/0004-6361/202140948>

D. Píša, J. Souček, O. Santolík, M. Hanzelka, G. Nicolaou, M. Maksimovic, S. D. Bale, T. Chust, Y. Khotyaintsev, V. Krasnoselskikh, M. Kretzschmar, E. Lorfèvre, D. Plettemeier, M. Steller, Š. Štverák, P. Trávníček, A. Vaivads, A. Vecchio, T. Horbury, H. O'Brien, V. Evans, V. Angelini, C. J. Owen and P. Louarn, First-year ion-acoustic wave observations in the solar wind by the RPW/TDS instrument on board Solar Orbiter, *A&A*, 656 (2021) A14, <https://doi.org/10.1051/0004-6361/202140928>

A. Zaslavsky, I. Mann, **J. Souček**, A. Czechowski, **D. Píša**, J. Vaverka, N. Meyer-Vernet, M. Maksimovic, E. Lorfèvre, K. Issautier, K. Rackovic Babic, S. D. Bale, M. Morooka, A. Vecchio, T. Chust, Y. Khotyaintsev, V. Krasnoselskikh, M. Kretzschmar, D. Plettemeier, M. Steller, Š. Štverák, P. Trávníček and A. Vaivads, First dust measurements with the Solar Orbiter Radio and Plasma Wave instrument, *A&A*, 656 (2021) A30, <https://doi.org/10.1051/0004-6361/202140969>

Related references:

M. Maksimovic, **J. Souček**, T. Chust, Y. Khotyaintsev, M. Kretzschmar, X. Bonnin, A. Vecchio, O. Alexandrova, S. D. Bale, D. Bérard, J.-Y. Brochot, N. J. T. Edberg, A. Eriksson, L. Z. Hadid, E. P. G. Johansson, T. Karlsson, B. Katra, V. Krasnoselskikh, V. Krupař, S. Lion, E. Lorfèvre, L. Matteini, Q. N. Nguyen, **D. Píša**, R. Piberne, D. Plettemeier, H. O. Rucker, **O. Santolík**, K. Steinvall, M. Steller, Š. Štverák, P. Trávníček, A. Vaivads, A. Zaslavsky, S. Chaintreuil, M. Dekkali, P.-A. Astier, G. Barbary, K. Boughedada, B. Cecconi, F. Chapron, C. Collin, D. Dias, L. Guéguen, L. Lamy, V. Leray, L. R. Malac-Allain, F. Pantellini, J. Parisot, P. Plasson, S. Thijs, I. Fratter, E. Bellouard, P. Danto, S. Julien, E. Guilhem, C. Fiachetti, J. Sanisidro, C. Laffaye, F. Gonzalez, B. Pontet, N. Quéruel, G. Jannet, P. Ferreau, T. Dudok de Wit, T. Vincent, C. Agrapart, J. Pragout, M. Bergerard-Timofeeva, G. T. Delory, P. Turin, A. Jeandet, P. Leroy, J.-C. Pellion, V. Bouzid, W. Recart, **I. Kolmašová, O. Krupařová, L. Uhlíř, R. Lán, J. Baše**, M. André, L. Bylander, V. Cripps, C. Cully, S.-E. Jansson, W. Puccio, J. Břínek, H. Ottacher, V. Angelini, M. Berthomier, V. Evans, K. Goetz, P. Hellinger, T. S. Horbury, K. Issautier, E. Kontar, O. Le Contel, P. Louarn, M. Martinović, D. Müller, H. O'Brien, C. J. Owen, A. Retino, J. Rodríguez-Pacheco, F. Sahraoui, L. Sanchez, A. P. Walsh, R. F. Wimmer-Schweingruber and I. Zouganelis, First observations and performance of the RPW instrument on board the Solar Orbiter mission, *A&A*, 656 (2021) A41, <https://doi.org/10.1051/0004-6361/202141271>

D. B. Graham, Yu. V. Khotyaintsev, A. Vaivads, N. J. T. Edberg, A. I. Eriksson, E. P. G. Johansson, L. Sorriso-Valvo, M. Maksimovic, **J. Souček, D. Píša**, S. D. Bale, T. Chust, M. Kretzschmar, V. Krasnoselskikh, E. Lorfèvre, D. Plettemeier, M. Steller, Š. Štverák, P. Trávníček, A. Vecchio, T. S. Horbury, H. O'Brien, V. Evans and V. Angelini, Kinetic electrostatic waves and their association with current structures in the solar wind, *A&A*, 656 (2021) A23, <https://doi.org/10.1051/0004-6361/202140943>

R. Gómez-Herrero, D. Pacheco, A. Kollhoff, F. Espinosa Lara, J. L. Freiherr von Forstner, N. Dresing, D. Lario, L. Balmaceda, V. Krupař, O. E. Malandraki, A. Aran, R. Bučík, A. Klassen, K.-L. Klein, I. Cernuda, S. Eldrum, H. Reid, J. G. Mitchell, G. M. Mason, G. C. Ho, J. Rodríguez-Pacheco, R. F. Wimmer-Schweingruber, B. Heber, L. Berger, R. C. Allen, N. P. Janitzek, M. Laurenza, R. De Marco, N. Wijsen, Y. Y. Kartavykh, W. Dröge, T. S. Horbury, M. Maksimovic, C. J. Owen, A. Vecchio, X. Bonnin, **O. Krupařová, D. Píša, J. Souček**, P. Louarn, A. Fedorov, H. O'Brien, V. Evans, V. Angelini, P. Zucca, M. Prieto, S. Sánchez-Prieto, A. Carrasco, J. J. Blanco, P. Parra, O. Rodríguez-Polo, C. Martín, J. C. Terasa, S. Boden, S. R. Kulkarni, A. Ravanbakhsh, M. Yedla, Z. Xu, G. B. Andrews, C. E. Schlemm, H. Seifert, K. Tyagi, W. J. Lees and J. Hayes, First near-relativistic solar electron events observed by EPD onboard Solar Orbiter, *A&A*, 656 (2021) L3, <https://doi.org/10.1051/0004-6361/202039883>

A. Vecchio, M. Maksimovic, **V. Krupar**, X. Bonnin, A. Zaslavsky, P. L. Astier, M. Dekkali, B. Cecconi, S. D. Bale, T. Chust, E. Guilhem, Yu. V. Khotyaintsev, V. Krasnoselskikh, M. Kretzschmar, E. Lorfèvre, D. Plettemeier, **J. Souček**, M. Steller, Š. Štverák, P. Trávníček and A. Vaivads, Solar Orbiter/RPW antenna calibration in the radio domain and its application to type III burst observations, *A&A*, 656 (2021) A33, <https://doi.org/10.1051/0004-6361/202140988>

Yu. V. Khotyaintsev, D. B. Graham, A. Vaivads, K. Steinvall, N. J. T. Edberg, A. I. Eriksson, E. P. G. Johansson, L. Sorriso-Valvo, M. Maksimovic, S. D. Bale, T. Chust, V. Krasnoselskikh, M. Kretzschmar, E. Lorfèvre, D. Plettemeier, **J. Souček**, M. Steller, Š. Štverák, P. Trávníček, A. Vecchio, T. S. Horbury, H. O'Brien, V. Evans and V. Angelini, Density fluctuations associated with turbulence and waves - First observations by Solar Orbiter, *A&A*, 656 (2021) A19, <https://doi.org/10.1051/0004-6361/202140936>

F. Carbone, L. Sorriso-Valvo, Yu. V. Khotyaintsev, K. Steinvall, A. Vecchio, D. Telloni, E. Yordanova, D. B. Graham, N. J. T. Edberg, A. I. Eriksson, E. P. G. Johansson, C. L. Vásconez, M. Maksimovic, R. Bruno, R. D'Amicis, S. D. Bale, T. Chust, V. Krasnoselskikh, M. Kretzschmar, E. Lorfèvre, D. Plettemeier, **J. Souček**, M. Steller, Š. Štverák, P. Trávníček, A. Vaivads, T. S. Horbury, H. O'Brien, V. Angelini and V. Evans, Statistical study of electron density turbulence and ion-cyclotron waves in the inner heliosphere: Solar Orbiter observations, *A&A*, 656 (2021) A16, <https://doi.org/10.1051/0004-6361/202140931>

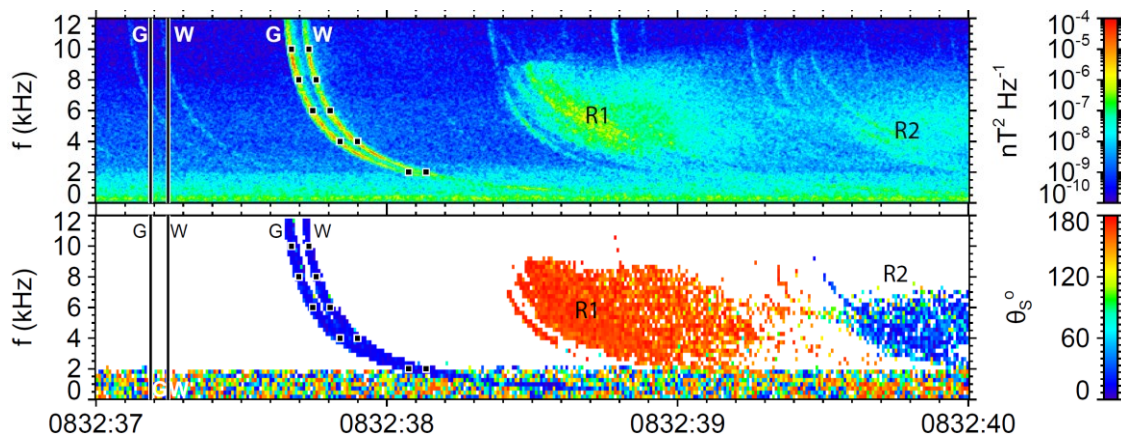
K. Steinvall, Yu. V. Khotyaintsev, G. Cozzani, A. Vaivads, E. Yordanova, A. I. Eriksson, N. J. T. Edberg, M. Maksimovic, S. D. Bale, T. Chust, V. Krasnoselskikh, M. Kretzschmar, E. Lorfèvre, D. Plettemeier, **J. Souček**, M. Steller, Š. Štverák, A. Vecchio, T. S. Horbury, H. O'Brien, V. Evans, A. Fedorov, P. Louarn, V. Génot, N. André, B. Lavraud, A. P. Rouillard and C. J. Owen, Solar wind current sheets and deHoffmann-Teller analysis - First results from Solar Orbiter's DC electric field measurements, *A&A*, 656 (2021) A9, <https://doi.org/10.1051/0004-6361/202140855>

D. Telloni, C. Scolini, C. Möstl, G. P. Zank, L.-L. Zhao, A. J. Weiss, M. A. Reiss, R. Laker, D. Perrone, Y. Khotyaintsev, K. Steinvall, L. Sorriso-Valvo, T. S. Horbury, R. F. Wimmer-Schweingruber, R. Bruno, R. D'Amicis, R. De Marco, V. K. Jagarlamudi, F. Carbone, R. Marino, M. Stangalini, M. Nakanotani, L. Adhikari, H. Liang, L. D. Woodham, E. E. Davies, H. Hietala, S. Perri, R. Gómez-Herrero, J. Rodríguez-Pacheco, E. Antonucci, M. Romoli, S. Fineschi, M. Maksimovic, **J. Souček**, T. Chust, M. Kretzschmar, A. Vecchio, D. Müller, I. Zouganelis, R. M. Winslow, S. Giordano, S. Mancuso, R. Susino, S. L. Ivanovski, M. Messerotti, H. O'Brien, V. Evans and V. Angelini, Study of two interacting interplanetary coronal mass ejections encountered by Solar Orbiter during its first perihelion passage - Observations and modeling, *A&A*, 656 (2021) A5, <https://doi.org/10.1051/0004-6361/202140648>

P. Kajdič, Y. Pfau-Kempf, L. Turc, A. P. Dimmock, M. Palmroth, K. Takahashi, E. Kilpua, **J. Souček**, N. Takahashi, L. Preisser, X. Blanco-Cano, D. Trotta, D. Burgess (2021), ULF Wave Transmission Across Collisionless Shocks: 2.5D Local Hybrid Simulations, *Journal of Geophysical Research: Space Physics*, 126, e2021JA029283. <https://doi.org/10.1029/2021JA029283>

2. Multipoint measurements of whistler-mode waves in the Earth's magnetosphere: hiss originating in whistlers

Measurements of electromagnetic waves in space plasmas are an important tool for our understanding of physical processes in this environment. We used multi-point measurements of electromagnetic field fluctuations by the Cluster space fleet to discuss sources of plasmaspheric hiss. Our case study shows hiss which was triggered in the dayside outer plasmasphere by unducted whistlers emitted from strong lightning strokes. Spectral properties of magnetospherically reflecting whistlers and hiss strongly depend on geographical location of the source. We also showed results collected during a close conjunction of the Van Allen Probes and Arase spacecraft. The inter-calibration was based on a fortuitous case of common observations of strong whistlers at frequencies between a few hundred hertz and 10 kHz, which were generated by the same lightning strokes and which propagated along very similar paths to the two spacecraft.



Observations of strong whistlers by the Van Allen Probe B spacecraft. Top: total power spectral density of magnetic field fluctuations obtained as the trace of the magnetic spectral matrix; bottom: angle between the spectral estimate of the Poynting vector and the vector of the background magnetic field.

References:

- Santolík, O., Kolmašová, I.,** Pickett, J. S., & Gurnett, D. A. (2021). Multi-point observation of hiss emerging from lightning whistlers. *Journal of Geophysical Research: Space Physics*, 126, e2021JA029524. <https://doi.org/10.1029/2021JA029524>
- Santolík, O.,** Miyoshi, Y., **Kolmašová, I.,** Matsuda, S., Hospodarsky, G. B., Hartley, D. P., et al. (2021). Inter-calibrated measurements of intense whistlers by Arase and Van Allen Probes. *Journal of Geophysical Research: Space Physics*, 126, e2021JA029700. <https://doi.org/10.1029/2021JA029700>

Related references:

Němec, F., Hajoš, M., Parrot, M., & Santolík, O. (2021). Quasiperiodic emissions and related particle precipitation bursts observed by the DEMETER spacecraft. *Journal of Geophysical Research: Space Physics*, 126, e2021JA029621. <https://doi.org/10.1029/2021JA029621>

Martinez-Calderon, C., Katoh, Y., Manninen, J., Santolík, O., Kasahara, Y., Matsuda, S., et al. (2021). Multi-event study of characteristics and propagation of naturally occurring ELF/VLF waves using high-latitude ground observations and conjunctions with the Arase satellite. *Journal of Geophysical Research: Space Physics*, 126, e2020JA028682. <https://doi.org/10.1029/2020JA028682>

Millan, R. M., Ripoll, J-F., Santolík, O., Kurth, W. S. (2021). Early-time Non-equilibrium Pitch Angle Diffusion of Electrons by Whistler-mode Hiss in a Plasmaspheric Plume Associated with BARREL Precipitation. *Front. Astron. Space Sci.* 8, 776992. <https://doi.org/10.3389/fspas.2021.776992>

Němec, F., Santolík, O., & Parrot, M. (2021). Doppler shifted Alpha transmitter signals in the conjugate hemisphere: DEMETER spacecraft observations and raytracing modeling. *Journal of Geophysical Research: Space Physics*, 126, e2020JA029017. <https://doi.org/10.1029/2020JA029017>

Pierrard, V., Ripoll, J.-F., Cunningham, G., Botek, E., Santolík, O., Thaller, S., et al. (2021). Observations and simulations of dropout events and flux decays in October 2013: Comparing MEO equatorial with LEO polar orbit. *Journal of Geophysical Research: Space Physics*, 126, e2020JA028850. <https://doi.org/10.1029/2020JA028850>

Ripoll, J.-F., M.H. Denton, D.P. Hartley, G.D. Reeves, D. Malaspina, G.S. Cunningham, O. Santolík, S.A. Thaller, V. Loidan, J.F. Fennell, D.L. Turner, W.S. Kurth, C.A. Kletzing, M.G. Henderson, A.Y. Ukhorskiy (2021), Scattering by whistler-mode waves during a quiet period perturbed by substorm activity, *Journal of Atmospheric and Solar-Terrestrial Physics* 215, 105471, <https://doi.org/10.1016/j.jastp.2020.105471>.

3. The Faraday rotation effect in Saturn Kilometric Radiation observed by the Cassini spacecraft

Non-thermal radio emissions from Saturn, known as Saturn Kilometric Radiation (SKR), were analyzed for the Faraday rotation effect detected in Cassini RPWS High Frequency Receiver (HFR) observations. This phenomenon, which mainly affects the lower-frequency part of SKR below 200 kHz, is characterized by a rotation of the semi-major axis of the SKR polarization ellipse as a function of frequency during wave propagation through a birefringent plasma medium. Faraday rotation was found in 4.1% of all HFR data recorded by Cassini above 20 degrees northern and southern magnetic latitude, from mid-2004 to late 2017. A statistical visibility analysis has shown that elliptically polarized SKR from the dawn source regions, when beamed toward high latitudes into the noon and afternoon local time sectors, is most likely to experience Faraday rotation along the ray path. The necessary conditions for Faraday rotation were discussed in terms of birefringent media and sharp plasma density gradients, where SKR (mostly R-X mode) gets split into the two circularly polarized modes R-X and L-O. By means of a case study we also demonstrated how Faraday rotation provides an estimate for the average plasma density along the ray path.

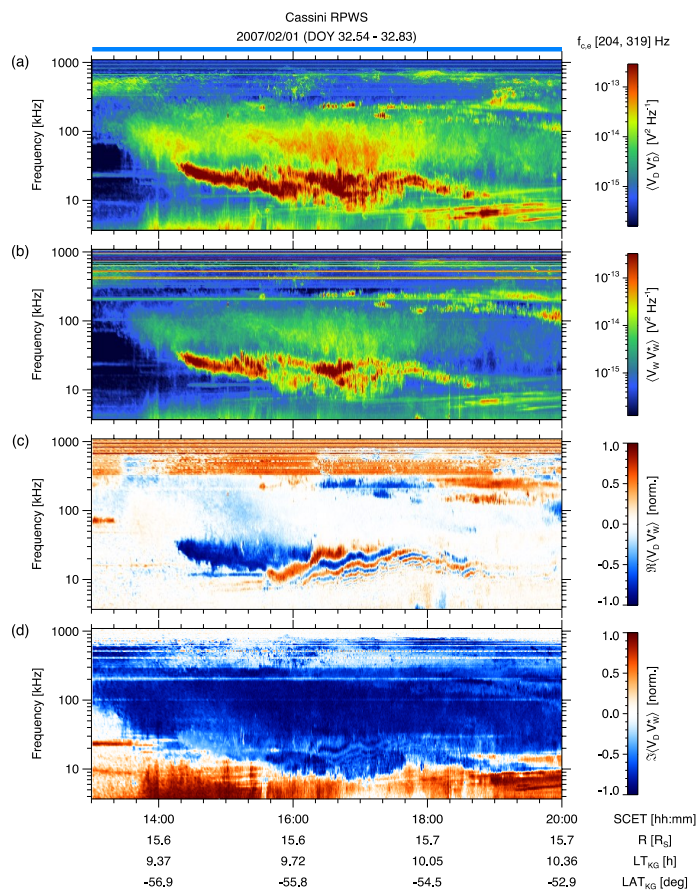
Reference:

Taubenschuss, U., Lamy, L., Fischer, G., **Piša, D., Santolík, O., Souček, J.,** Kurth, W. S., Cecconi, B., Zarka, P., Rucker, H. O. (2021). The Faraday rotation effect in Saturn Kilometric Radiation observed by the CASSINI spacecraft. *Icarus*, 370, 114661. <https://doi.org/10.1016/j.icarus.2021.114661>

Related references:

Menietti, J. D., Averkamp, T. F., Kurth, W. S., Imai, M., Faden, J. B., Hospodarsky, G. B., **Santolik, O.,** Clark, G., Allegrini, F., Elliott, S. S., Sulaiman, A. H., Bolton, S. J. (2021). Analysis of Whistler-Mode and Z-Mode Emission in the Juno Primary Mission. *Journal of Geophysical Research: Space Physics*, Volume 126, e29885. <https://doi.org/10.1029/2021JA029885>

Goetz, C., Gunell, H., Volwerk, M., A. Beth, A. Eriksson, M. Galand, P. Henri, H. Nilsson, C. Simon Wedlund, M. Alho, L. Andersson, N. Andre, J. De Keyser, J. Deca, Y. Ge, K.-H. Glassmeier, R. Hajra, T. Karlsson, S. Kasahara, **I. Kolmasova,** K. Llera, H. Madanian, I. Mann, C. Mazelle, E. Odelstad, F. Plaschke, M. Rubin, B. Sanchez-Cano, C. Snodgrass & E. Vigren, Cometary plasma science. *Exp Astron* (2021). <https://doi.org/10.1007/s10686-021-09783-z>



A summary of Cassini RPWS/HFR observations in 2-antenna mode from February 1, 2007. (a) Auto-power spectral density in the dipole antenna, (b) auto-power spectral density in the w-antenna, (c) real part (including Faraday fringes) and (d) imaginary part of the cross-power spectral density between both antennas. Time and spacecraft coordinates (cronographic) are given at the bottom. Modulations of SKR emission by Faraday rotation are clearly visible in (c) between 7 and 30 kHz as oscillations of $Re\langle V_D V_w^ \rangle$ between -1 (blue) and +1 (red).*

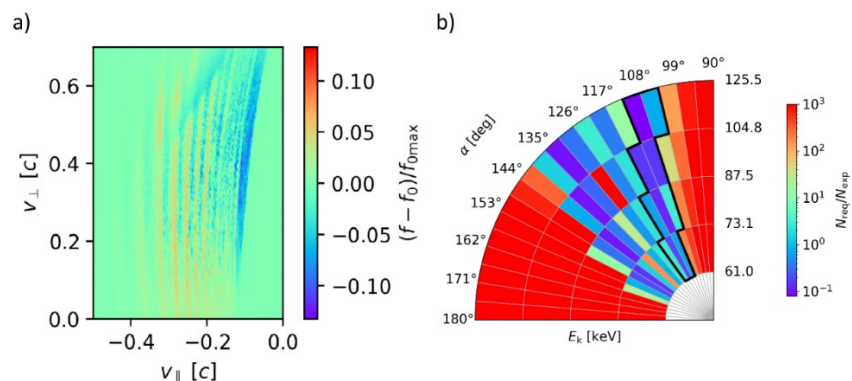
4. Measurability of the nonlinear response of electron distribution function to chorus emissions in the Earth's radiation belt

The whistler-mode chorus waves are known to have a major impact on the dynamics of the Earth's outer radiation belt, causing acceleration and loss of energetic electrons. In this paper we focused on the possibility of analyzing the nonlinear properties of chorus through measurements of perturbations in the hot electron velocity distribution caused by interaction with the waves. We used a recently developed model of a single rising-tone chorus element with a subpacket structure and employed backward-in-time test particle simulations to obtain the perturbed electron distribution. We then analyzed the character and magnitude of these perturbations and assessed their measurability.

It was found that the nonlinear interaction of chorus subpackets with electrons causes the creation of stripes of increased and decreased phase space density. These stripes are initially aligned to resonance velocity curves, but become distorted due to the adiabatic motion of the electrons, and their structure further becomes less clear as the frequency of the chorus riser increases. On the front of the perturbation region, a prominent decrease in phase space density, associated with the electromagnetic electron hole, can be observed. We calculated the particle fluxes in our simulation and estimated the particle counts which could be measured by the state-of-art electrostatic analyzers on spacecraft. We concluded that no recent particle instrument has the necessary pitch angle resolution and geometric factor to make a significant observation. A new instrument with improved angular resolution is needed to measure the perturbations predicted by our simulations. A successful observation would confirm the validity of previous theoretical predictions, and it could also partially reconcile two major theories of chorus growth, the nonlinear growth theory and the backward-wave oscillator theory.

Reference:

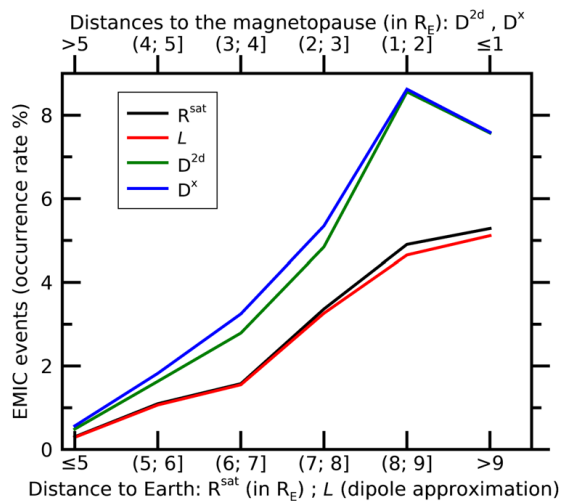
Hanzelka, M., Santolík, O., Omura, Y., & Kolmašová, I. (2021). Measurability of the nonlinear response of electron distribution function to chorus emissions in the Earth's radiation belt. *Journal of Geophysical Research: Space Physics*, 126, e2021JA029624. <https://doi.org/10.1029/2021JA029624>



a) Perturbations of hot electron velocity distribution after interaction with a chorus element, as captured at the magnetic equator right after the last subpacket. The plot shows a normalized difference between the perturbed distribution and the initial distribution. b) Polar plot in energy-pitch angle space showing the ratio N_{req}/N_{exp} , where N_{req} is the number of particles required to make a 1-sigma significant measurement of the perturbations, and N_{exp} is the number of particles expected to be measured by an electrostatic particle analyzer.

5. Occurrence of electromagnetic ion cyclotron waves in the magnetosphere according to their distance to the magnetopause

Wave growth of electromagnetic ion cyclotron (EMIC) emissions observed in the outer magnetosphere is mainly controlled by compression events resulting from solar wind dynamic pressure pulses. During such events wave growth is expected to be maximum close to the magnetopause. In previous studies, distribution of EMIC waves was analyzed according to their distance from the Earth, which is inadequate for studying the magnetopause region. We mapped a data set of EMIC waves observed by the THEMIS spacecraft according to their distance from a case-by-case modeled magnetopause. EMIC occurrence rate was found to be maximum within two Earth radii from the magnetopause and then it linearly decreased with the increasing distance, especially close to the local noon.



Occurrence rate (right panel) of EMIC events observed up to 10 Earth radii (RE) between 8 and 16 MLT, by the THEMIS spacecraft. Results are presented as a function of L (in red), the distance to Earth R^{sat} (in black) or to the modelled magnetopause (absolute distance D^{2d} in green and distance toward the Sun D^x in blue). Upper and lower abscissa have opposite orientations to make comparisons easier.

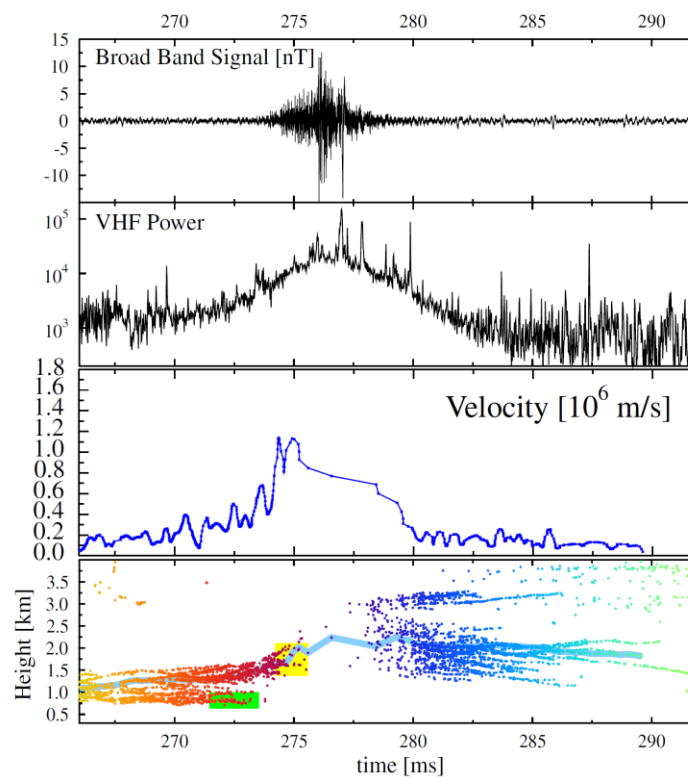
Reference:

Grison, B., Santolík, O., Lukačević, J., & Usanova, M. E. (2021). Occurrence of EMIC waves in the magnetosphere according to their distance to the magnetopause. *Geophysical Research Letters*, 48, e2020GL090921. <https://doi.org/10.1029/2020GL090921>

6. Atmospheric electricity: A distinct negative leader propagation mode

We studied the atmospheric electricity phenomena from both small and large-scale perspectives. We investigated in detail the propagation of evolving lightning discharge inside thunderclouds (Scholten et al, 2021a, b). We also introduced a new method for automated detection of atmospheric and tweak atmospheric. This method can be used for monitoring of diurnal, nocturnal and seasonal variations of the ionospheric D-layer (Maslej-Křešňáková et al, 2021).

We combined narrowband measurements made with the LOFAR (Low-Frequency Array) radio telescope, an instrument primarily built for radio-astronomy observations and the broadband magnetic field data recorded by the Shielded Loop Antenna with a Versatile Integrated Amplifier (SLAVIA) in order to investigate propagation of negative lightning leaders. We observed that a negative in-cloud leader rather suddenly changed, for a few milliseconds, into a mode where it radiated 100 times more very high frequency (VHF) power and propagated faster than typical negative leaders. After this rapid propagation mode, it spawned in a large number of more typical negative leaders. This rapid mode occurred during the initial stage of all (25) lightning flashes we have mapped. For some flashes this mode occurred also well after initiation and we showed one case where it was triggered twice, some 100 ms apart. We postulated that the rapid propagation mode was indicative of a small (order of 5 km²) but dense charge pocket in vicinity of which lightning appeared to be exclusively initiated.



a) Broadband magnetic field waveform, b) power recorded at a core station of LOFAR, c) propagation velocity along the track indicated in light blue in the panel d, d) VHF sources localized by LOFAR. The records started at 21:03:06.757 UTC on 19 April, 2019.

References:

Scholten, O., Hare, B.M., Dwyer, J., Liu, N., Sterpka, C., **Kolmašová, I., Santolík, O., Lán, R, Uhlíř, L**, et al., 2021: A distinct negative leader propagation mode, *Scientific Reports*, 11, 16256

Scholten, O., Hare, B. M., Dwyer, J., Sterpka, C., **Kolmašová, I., Santolík, O., Lán, R, Uhlíř, L**, et al., 2021: The initial stage of cloud lightning imaged in high-resolution, *Journal of Geophysical Research: Atmospheres*, 126,4, e2020JD033126

Maslej-Křešňáková, V., Kundrát, A., Mackovjak, Š., Butka, P., Jaščur, S., **Kolmašová, I., Santolík, O.**, 2021: Automatic detection of atmospheric and tweek atmospheric in radio spectrograms based on a deep learning approach, *Earth and Space Science*, 8, 11, e2021EA002007

Related references:

Chum, Jaroslav, Kollárik, M., **Kolmašová, I.**, Langer, R., Ruzs, Jan, Saxonbergová, Dana, Strhárský, I., 2021: Influence of Solar Wind on Secondary Cosmic Rays and Atmospheric Electricity, *Frontiers in Earth Science*, 9, 671801

Strumik, M., J. Slominski, E. Slominska, J. Mlynarczyk, J. Blecki, R. Haagmans, A. Kulak, **M. Popek**, K. Martynski, R. Wronowski (2021). Experimental evidence of a link between lightning and magnetic field fluctuations in the upper ionosphere observed by swarm. *Geophysical Research Letters*, 48, e2020GL091507. <https://doi.org/10.1029/2020GL091507>

7. Radio and plasma waves in the vicinity of Venus and whistler-mode waves in the solar wind.

On December 27, 2020, Solar Orbiter completed its first gravity assist maneuver of Venus. While this flyby was performed to provide the spacecraft with sufficient velocity to get closer to the Sun and observe its poles from progressively higher inclinations, the Radio and Plasma Wave (RPW) consortium, along with other operational in-situ instruments, had the opportunity to perform high cadence measurements and study the plasma properties in the induced magnetosphere of Venus (Hadid et al 2021). These observations include the identification of a number of magnetospheric plasma wave modes, measurements of the electron number densities computed using the quasi-thermal noise spectroscopy technique and inferred from the probe-to-spacecraft potential, the observation of dust impact signatures, kinetic solitary structures, and localized structures at the bow-shock, in addition to the validation of the wave normal analysis on-board from the Low Frequency Receiver. Our contribution to the development of algorithms for this module was also reflected by new results on the whistler mode waves in the solar wind (Chust et al, 2021; Kretzschmar et al, 2021).

Reference

L. Z. Hadid, N. J. T. Edberg, T. Chust, **D. Píša**, A. P. Dimmock, M. W. Morooka, M. Maksimovic, Yu. V. Khotyaintsev, **J. Souček**, M. Kretzschmar, A. Vecchio, O. Le Contel, A. Retino, R. C. Allen, M. Volwerk, C. M. Fowler, L. Sorriso-Valvo, T. Karlsson, **O. Santolík, I. Kolmašová**, F. Sahraoui, K. Stergiopoulou, X. Moussas, K. Issautier, R. M. Dewey, M. Klein Wolt, O. E. Malandraki, E. P. Kontar, G. G. Howes, S. D. Bale, T. S. Horbury, M. Martinović, A. Vaivads, V. Krasnoselskikh, E. Lorfèvre, D. Plettemeier, M. Steller, Š. Štverák, P. Trávníček, H. O'Brien, V. Evans, V. Angelini, M. C. Velli and I. Zouganelis, Solar Orbiter's first Venus flyby: Observations from the Radio and Plasma Wave instrument, *A&A*, 656 (2021) A18, <https://doi.org/10.1051/0004-6361/202140934>

Related references:

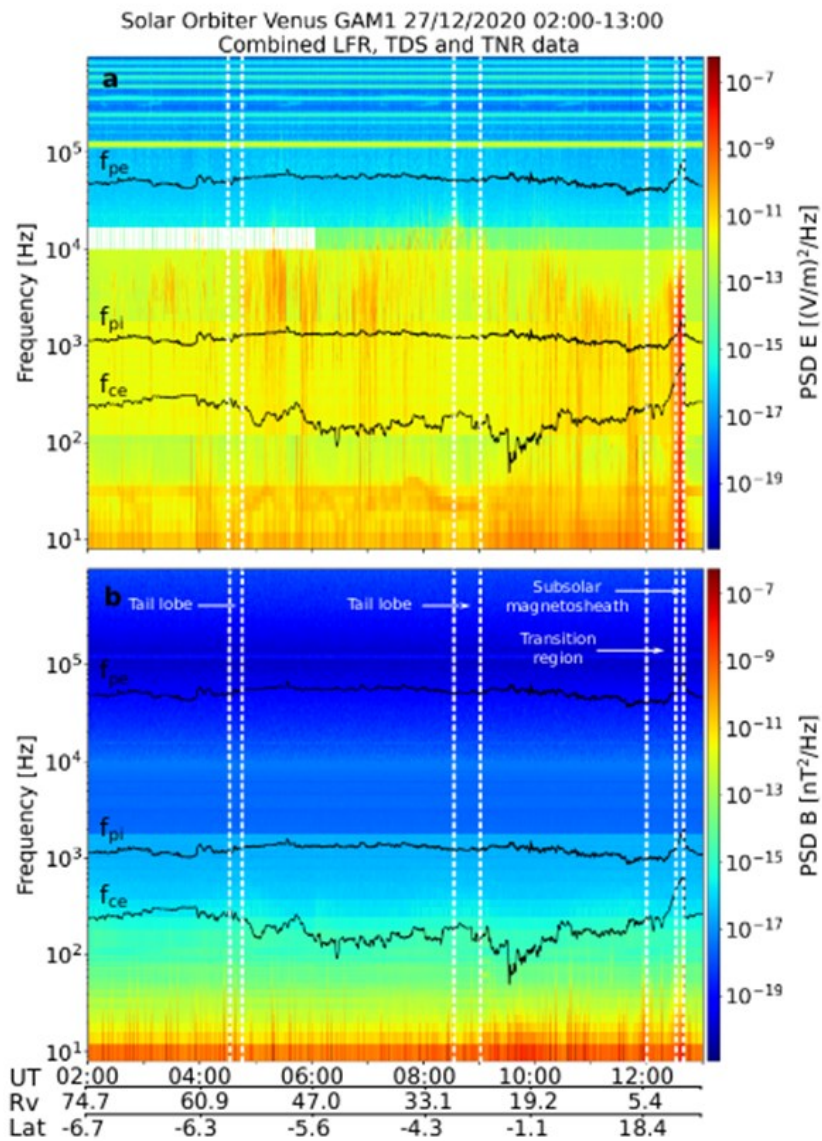
R. C. Allen, I. Cernuda, D. Pacheco, L. Berger, Z. G. Xu, J. L. Freiherr von Forstner, J. Rodríguez-Pacheco, R. F. Wimmer-Schweingruber, G. C. Ho, G. M. Mason, S. K. Vines, Y. Khotyaintsev, T. Horbury, M. Maksimovic, L. Z. Hadid, M. Volwerk, A. P. Dimmock, L. Sorriso-Valvo, K. Stergiopoulou, G. B. Andrews, V. Angelini, S. D. Bale, S. Boden, S. I. Böttcher, T. Chust, S. Eldrum, P. P. Espada, F. Espinosa Lara, V. Evans, R. Gómez-Herrero, J. R. Hayes, A. M. Hellín, A. Kollhoff, V. Krasnoselskikh, M. Kretzschmar, P. Kühl, S. R. Kulkarni, W. J. Lees, E. Lorfèvre, C. Martin, H. O'Brien, D. Plettemeier, O. R. Polo, M. Prieto, A. Ravanbakhsh, S. Sánchez-Prieto, C. E. Schlemm, H. Seifert, **J. Souček**, M. Steller, Š. Štverák, J. C. Terasa, P. Trávníček, K. Tyagi, A. Vaivads, A. Vecchio and M. Yedla, Energetic ions in the Venusian system: Insights from the first Solar Orbiter flyby, *A&A*, 656 (2021) A7, DOI: <https://doi.org/10.1051/0004-6361/202140803>

T. Chust, M. Kretzschmar, D. B. Graham, O. Le Contel, A. Retinò, A. Alexandrova, M. Berthomier, L. Z. Hadid, F. Sahraoui, A. Jeandet, P. Leroy, J.-C. Pellion, V. Bouzid, B. Katra, R. Piberne, Yu. V. Khotyaintsev, A. Vaivads, V. Krasnoselskikh, **J. Souček**, **O. Santolík**, E. Lorfèvre, D. Plettemeier, M. Steller, Š. Štverák, P. Trávníček, A. Vecchio, M. Maksimovic, S. D. Bale, T. S. Horbury, H. O'Brien, V. Evans and V. Angelini, Observations of whistler mode waves by Solar Orbiter's RPW Low Frequency Receiver (LFR): In-flight performance and first results, *A&A*, 656 (2021) A17 DOI: <https://doi.org/10.1051/0004-6361/202140932>

M. Kretzschmar, T. Chust, V. Krasnoselskikh, D. Graham, L. Colombari, M. Maksimovic, Yu. V. Khotyaintsev, **J. Souček**, K. Steinvall, **O. Santolík**, G. Jannet, J.-Y. Brochot, O. Le Contel, A. Vecchio, X. Bonnin, S. D. Bale, C. Froment, A. Larosa, M. Bergerard-Timofeeva, P. Fergeau, E. Lorfèvre, D. Plettemeier, M. Steller, Š. Štverák, P. Trávníček, A. Vaivads, T. S. Horbury, H. O'Brien, V. Evans, V. Angelini, C. J. Owen and P. Louarn, Whistler waves observed by Solar Orbiter/RPW between 0.5 AU and 1 AU, *A&A*, 656 (2021) A24, DOI: <https://doi.org/10.1051/0004-6361/202140945>

V. Génot, E. Budnik, C. Jacquy, M. Bouchemit, B. Renard, N. Dufourg, N. André, B. Cecconi, F. Pitout, B. Lavraud, A. Fedorov, M. Ganfloff, I. Plotnikov, R. Modolo, N. Lormant, H. Si Hadj Mohand, C. Tao, B. Besson, D. Heulet, D. Boucon, J. Durand, N. Bourrel, Q. Brzustowski, N. Jourdane, R. Hitier, P. Garnier, **B. Grison**, N. Aunai, A. Jeandet, F. Cabrolie, *Automated Multi-Dataset Analysis (AMDA): An on-line database and analysis tool for heliospheric and planetary plasma data*, *Planetary and Space Science*, Volume 201, 2021, 105214, ISSN 0032-0633, <https://doi.org/10.1016/j.pss.2021.105214>.

E. Chané, B. Schmieder, S. Dasso, C. Verbeke, **B. Grison**, P. Démoulin and S. Poedts, Over-expansion of a coronal mass ejection generates sub-Alfvénic plasma conditions in the solar wind at Earth, *A&A*, 647 (2021) A149, DOI: <https://doi.org/10.1051/0004-6361/202039867>



Overview of the combined power spectral densities observed by Solar Orbiter's radio and plasma wave instrument during its first flyby at Venus. (a) The electric field spectrum, obtained by combining RPW subsystems data from LFR, TDS and TNR. (b) The magnetic field spectrum, obtained by combining RPW subsystems data from LFR and TDS. The electron cyclotron (f_{ce}) and ion (f_{pi}) and electron plasma (f_{pe}) frequencies are shown in black lines ($f_{ce} < f_{pi} < f_{pe}$). The vertical dashed lines delimit different regions in the induced magnetosphere of Venus.

Department of Space Physics, Institute of Atmospheric Physics of the Czech Academy of Sciences in 2021

1. Radka Balková, secretary, 50% FTE
2. Sampath Bandara, postdoctoral associate, since July 16, 2021
3. Zdeněk Griehl, technician, 40% FTE
4. Benjamin Grison, research scientist
5. Michajlo Hajoš, research scientist
6. Miroslav Hanzelka, PhD student, 70% FTE
7. Jiří Jánský, research engineer
8. Petr Kašpar, research scientist
9. Ivana Kolmašová, senior research scientist
10. Andrea Kolínská, PhD student, 70% FTE
11. *Vratislav Krupař, research scientist, on leave*
12. *Oksana Krupařová, research scientist, on leave*
13. Radek Lán, research engineer
14. Jan Lukačevič, PhD student, 70% FTE, *until January 31, 2021*
15. David Píša, research scientist
16. Martin Popek, TLE observer, 25% FTE
17. Ondřej Santolík, senior research scientist, head of the department
18. Jan Snížek, research engineer, 50% FTE
19. Jan Souček, senior research scientist, deputy head of the department
20. Hana Špačková, PhD student, 70% FTE, *on leave since September 20, 2021*
21. Ulrich Taubenschuss, research scientist
22. *Alexander Tomori, PhD student, on leave*
23. Marie Turčičová, PhD student, since April 6, 2021
24. Luděk Uhlíř, research engineer